Adiponectin inhibits hepatic stellate cell activation by targeting the PTEN/AKT pathway

Pradeep Kumar[a,*], **Reben Raeman**[c], **Daniel M. Chopyk**[a], **Tekla Smith**[a], **Kiran Verma**[b], **Yunshan Liu**[a], and **Frank A. Anania**[a]

[a]Division of Digestive Diseases, Department of Medicine, Emory University, Atlanta, GA, USA

[b]Labratory of Biochemical Pharmacology, Department of Pediatrics, Emory University, Atlanta, GA, USA

[c]Department of Pathology, University of Pittsburgh, Pittsburgh, PA, USA

Abstract

Adiponectin inhibits hepatic stellate cell (HSC) activation and subsequent development of liver fibrosis via multiple mechanisms. Phosphatase and tensin homolog deletion 10 (PTEN) plays a crucial role in suppression of HSC activation, but its regulation by adiponectin is not fully understood. Here, we investigated the effect of adiponectin on PTEN in LX-2 cells, a human cell line and examined the underlying molecular mechanisms involved in adiponectin-mediated upregulation of PTEN activity during fibrosis. PTEN expression was found to be significantly reduced in the livers of mice treated with CCl_4, whereas its expression was rescued by adiponectin treatment. The DNA methylation proteins DNMT1, DNMT3A, and DNMT3B are all highly expressed in activated primary HSCs compared to quiescent HSCs, and thus represent additional regulatory targets during liver fibrogenesis. Expression of DNMT proteins was significantly induced in the presence of fibrotic stimuli; however, only DNMT3B expression was reduced in the presence of adiponectin. Adiponectin-induced suppression of DNMT3B was found to be mediated by enhanced miR-29b expression. Furthermore, PTEN expression was significantly increased by overexpression of miR-29b, whereas its expression was markedly reduced by a miR-29b inhibitor in LX-2 cells. These findings suggest that adiponectin-induced upregulation of miR-29b can suppress DNMT3B transcription in LX-2 cells, thus resulting in reduced methylation of PTEN CpG islands and ultimately suppressing the PI3K/AKT pathway. Together, these data suggest a possible new explanation for the inhibitory effect of adiponectin on HSC activation and liver fibrogenesis.

Keywords

Liver fibrosis; Adiponectin; PTEN; DNA methylation; microRNA

[*]Corresponding author at: Division of Digestive Disease, Department of Medicine, 615 Michael Street, Room 275, Atlanta, GA 30322, USA. pkuma23@emory.edu (P. Kumar).

1. Introduction

Hepatic fibrosis is a reversible wound-healing process characterized by excessive deposition of extracellular matrix (ECM) proteins, especially fibrillar collagen [1,2]. Fibrosis is a consequence of chronic injury associated with alcoholic liver disease (ALD), non-alcoholic fatty liver disease (NAFLD) as well as chronic viral diseases such as hepatitis C viral infection [3,4]. Hepatic stellate cells (HSCs) are the primary players in hepatic fibrosis development and progression [5]. When activated, HSCs transdifferentiate into α-smooth muscle actin (α-SMA) expressing myofibroblast-like cells, which are the major matrix-producing cells involved in hepatic fibrosis [1]. We and others have recently demonstrated that adiponectin, a 30 kDa adipocytokine primarily secreted by white adipose tissue (WAT), has anti-fibrotic properties both in vivo and in vitro [6–10]. Adiponectin signaling occurs via its two cognate receptors: adiponectin receptor 1 and 2 [11,12]. However, the molecular mechanism responsible for anti-fibrotic effects induced by adiponectin remained unexplored.

The phosphatase and tensin homolog deleted on chromosome 10 (PTEN) is a dual phosphatase, and its major function is to dephosphorylate phosphatidylinositol 3, 4, 5−triphosphate (PIP3) to phosphatidylinositol 4, 5−bisphosphate [13]. Decreased PTEN expression has been reported in fibrotic diseases of the lungs, heart, skin as well as liver [14–18]. Specifically, deletion of the *Pten* gene in mice results in excess deposition of type I collagen, while PTEN overexpression can reverse chemical-induced liver fibrosis [19]. PTEN activity and expression is controlled by several mechanisms including phosphorylation, acetylation, oxidation, ubiquitination, non-coding RNAs, and DNA methylation [20–22]. For instance, aberrant PTEN promoter methylation is demonstrated in CCl_4-induced liver fibrosis [23]. DNA methylation is mainly carried out by three highly conserved enzymes, DNMT1, DNMT3A, and DNMT3B [24].

Recent studies indicate that aberrant microRNA (miRNA) expression is correlated with liver fibrosis [25,26]. miRNAs are a class of endogenous small non-coding RNAs that are typically 18–22 nucleotides in length [25]. These miRNAs typically work as posttranscriptional regulators of gene expression by binding with a portion of the 3′-untranslated-region (3′-UTR) of target mRNAs resulting in degradation or inhibition of the target mRNAs and thus initiation of translation [27]. miRNAs play critical roles in developmental and cellular processes such as growth, differentiation, apoptosis, and oncogenesis [28].

In the setting of liver fibrosis, miR-19, miR-29, and let-7 overexpression reduce α-SMA and collagen type I expression [29–31]. Additionally, miR-33a and miR-181b inhibitors reduce collagen type I and α-SMA expression in HSCs [21,32]. Moreover, published reports demonstrate that PTEN expression is tightly regulated by miR-29b in addition to DNMT3B [33]. However, how adiponectin modulates PTEN promoter methylation and miR-29b expression has not yet been fully described. Here, we hypothesized that adiponectin may play a role as an upstream regulator of PTEN expression via either DNMTs, miR-29b, or both. Hence this study aimed to investigate the molecular mechanisms underlying

adiponectin-mediated increased PTEN expression as a novel pathway in targeting liver fibrosis.

2. Materials and methods

2.1. Materials

Dulbecco's modified Eagle's medium (DMEM), trypsin-EDTA, and penicillin-streptomycin were all purchased from Invitrogen® (Carlsbad, CA). Fetal bovine serum (FBS) was purchased from Atlanta Biologicals, GA. Recombinant TGFβ1 was purchased from R&D systems (Minneapolis, MN). Recombinant high molecular weight (HMW) human adiponectin was purchased from Biovendor (Candler, NC). Antibodies p-AKT, AKT, PTEN, DNMT1, DNMT3A and DNMT3B were purchased from Cell Signaling (Danvers, MA). CCl_4 and antibodies against α-SMA and anti-β-actin were obtained from Sigma-Aldrich (St. Louis, MO). Collagen type I antibody was purchased from Abcam (Cambridge, MA).

2.2. Animals and CCl$_4$-induced liver fibrosis in mice

Eight-week -old male C57BL/6 J mice were purchased from Jackson Laboratories for animal studies (Bar Harbor Maine; Stock no. 000664). Animals were cared for in accordance to protocols approved by the Animal Care and Use Committee of Emory University. All animals were housed in a temperature-controlled environment with a 12:12 h light/ dark cycle. Animals were fed ad libitum with Purina Laboratory Chow (Ralston Purina, St. Louis, MO) and water. The study included three groups of mice: (I) Control mice that received olive oil by gavage and saline injections; (II) mice gavaged with CCl_4 and injected with a recombinant deficient adenovirus vector carrying E. coli β-galactosidase gene (Ad-LacZ); and (III) mice gavaged with CCl_4 and administered the recombinant deficient adenoviral vector carrying the human full-length adiponectin cDNA under the regulation of the CMV promoter (Ad-Adipo). Mice weighing 22–25 g were gavaged with olive oil as control or CCl_4 (1:1 ratio CCl_4 to oil; 2 ml/kg for both groups) thrice weekly for 6 weeks. Mice were given viral particle via tail vein injection (Ad-LacZ or Ad-Adipo (1×10^9 viral particles)) every third day for two weeks following 4 weeks of CCl_4 gavage. Saline was injected via tail vein in the control group. We measured serum adiponectin concentration following Ad-Adipo injection as previously described [7] (mouse adiponectin ELISA kit; Millipore, Billerica, MA, USA). Human adiponectin (NM_004797) containing adenovirus (Ad-Adipo) and Ad-LacZ were propagated in AD293 cells (Stratagene, La Jolla, CA). Adenoviruses were concentrated and purified with an Adeno-X virus purification kit (Clonetech Laboratories, Mountain View, CA), and viral titers were determined with Adeno-XMT rapid titer kit (Clonetech Laboratories).

2.3. Serum alanine aminotransferase (ALT) and aspartate aminotransferase (AST)

Serum ALT and AST levels were determined with an ALT and AST activity assay kit as per manufacturer's instruction (Sigma-Aldrich, St. Louis, MO).

2.4. Picrosirius red staining and quantification

Formalin-fixed, paraffin-embedded liver sections (5 μm) were deparaffinized and washed with double distilled water. Deparaffinized sections were incubated for 60 min with Sirius

red solution (Abcam, Cambridge, MA) followed by brief rinses with acetic acid (0.05%). Sections were dehydrated by washing with absolute alcohol. Sections were observed under a light microscope (Axioplan2; Carl Zeiss, Hallbergmoos, Germany). The collagen staining was quantified by using Image J software (NIH, Bethesda).

2.5. RNA extraction and qRT-PCR analysis

Total RNA was extracted from liver tissue or LX-2 cells using the RNeasy Mini Kit (Qiagen, Valencia, CA), and one microgram of total RNA was reverse transcribed to cDNA using the Bio-Rad's iScript™ cDNA synthesis kit according to the manufacturer's instructions. Gene expression was measured with real-time PCR using IQ™ SYBR® Green Supermix (Bio-Rad) according to standard protocol. All human and mouse primers were purchased from Sigma-Aldrich (St. Louis, MO, USA). The following primers were used in this study: mouse PTEN (NM_008960): forward 5′-TGGATTCGACTTAGACTTGACCT-3′ and re-verse 5′-GCGGTGTCATAATGTCTCTCAG-3′; mouse DNMT1 (NM_001199433) forward 5′-CCGTGGCTACGAGGAGAAC-3′ and re-verse 5′-CCGTGGCTACGAGGAGAAC-3′; mouse DNMT3A (NM_007872) forward 5′-GATGAGCCTGAGTATGAGGATGG-3′ and reverse 5′-CAAG ACACAATTCGGCCTGG-3′; mouse DNMT3B (NM_001122997) forward 5′-CGTTAATGGGAACTTCAGTGACC-3′ and reverse 5′-CTGCGTGTAAT TCAGAAGGCT-3′; mouse Acta2 (NM_007392) forward 5′-CCCAGACA TCAGGGAGTAATGG-3′ and reverse 5′-TCTATCGGATACTTCAGCG TCA-3′; human PTEN (NM_000314) Forward 5′-TGGATTCGACTTAGA CTTGACCT-3′ and reverse 5′-GGTGGGTTATGGTCTTCAAAAGG-3′. To detect the expression of miR-29b (Accession MIMAT0000100) 5′-CGC TAGCACCATTTGAAATCAG-3′, RT PCR was performed using the Quanta bio microRNA assay (Beverly, MA) according to user manual. The assays were performed in triplicate using the Mastercycler® eprealplex (Eppendorf®), with internal controls (18 s) for the expression of mRNA and U6 for miR-29b. The cycle threshold (Ct) values were normalized to reference gene 18 s/U6 and fold changes in expression were calculated using the $2^{-\text{Ct}}$ method.

2.5.1. Isolation of rat hepatic stellate cells—Primary rat HSCs were isolated from Male Sprague-Dawley® rats as previously described [7].

2.6. Cell lines

Human LX-2 cells, an immortalized human-derived cell line was a kind gift from Dr. Scott Friedman (Mount Sinai Hospital, New York).

2.7. Transient transfection of miRNA inhibitors and mimics

LX-2 cells were seeded in 6-wells plate (2×10^5 cells/well) for overnight and then transfected with a miR-29b inhibitor (Cat. HSTUD0436 Sigma), miR-29b mimic (Cat. HMI0436, Sigma) and respective controls (Sigma) for 24 h using the Lipofectamine™ RNAiMAX transfection reagent per manufacturer's instructions (Invitrogen, Carlsbad, CA).

2.8. Cell proliferation assay

Cells were plated at a density of 1×10^5 per well in 96-well plates and incubated at 37 °C with 5% CO_2 in a humidified incubator. After 24 h, cells were incubated with 100 μl of CellTiter 96® AQueous One Solution reagent (Promega Corporation, Madison, WI, USA) for an additional 4 h at 37 °C with 5% CO_2 in a humidified incubator. The absorbance at 490 nm was measured on a BioTek Synergy™ 2 plate reader (BioTek Instruments, Inc., Winooski, VT, USA).

2.9. Western blot assay

Protein concentration was quantified using a bicinchoninic acid (BCA) protein assay kit (ThermoFisher, Waltham, MA) and boiled in 1× Lamellae buffer (Bio-Rad) for 5 min in a heat block. Ten to thirty micrograms of total protein was subjected to sodium dodecyl sulfate-polyacrylamide gel electrophoresis (SDS-PAGE) and then transferred to 0.45 μm nitrocellulose membrane. The membranes were incubated with 5% non-fat dry milk followed by incubation with the primary antibody (1:1000) in 5% BSA for overnight at 4 °C. The membranes were washed with Tris-buffered saline tween followed by incubation with horse-radish peroxidase-conjugated secondary antibody (1:5000) for 1 h at room temperature. Protein bands were visualized using a HyGLO™ Chemiluminescent HRP Antibody Detection Reagent (Denville Scientific, NJ) and exposed to X-ray film (Kodak, Rochester, NY). Densitometric analysis of resolved proteins was performed to quantify protein band intensity with AlphaEaseFC™ Software, version 4.0.1 (Alpha Innotech, San Leandro, CA).

2.10. Genomic DNA isolation and methylation-specific polymerase chain assay (MS-PCR)

Genomic DNA was isolated using QIAGEN Genomic DNA purification kit (QAIGEN, Valencia, CA). For bisulfite treatment, EZ DNA methylation™ kit was used. Briefly, a total of 500 ng genomic DNA (50 μl) was incubated with 100 μl of CT conversion buffer followed by incubation in a thermal cycler at 50 °C for 12 h. The DNA was purified by using Zymo-spin™ IC column and eluted in 10 μl of elution buffer according to the user manual. After DNA purification, the methylated genomic DNA was subjected to PCR amplification. An MS-PCR assay was performed in a total volume of 20 μl by using SeqAMP DNA poly-merase (Takara, Mountain View, CA) as per user manual. The oligo-nucleotide sequences used for the MSP were: mouse PTEN U forward: 5′-TTGGAGTATTGATTAAGGTGG-3′; mouse PTEN U reverse: 5′-CAAT ATATCCACAACTCACTCCC-3′; mouse PTEN M forward: 5′-TTCGGAGT ATCGATTAAGGC-3′; mouse PTEN M reverse: 5′-AATATATCCGCGACT CGCTC-3′; human PTEN U forward: 5′-AATTGATTTGGAGTTTGAGG-3′; human PTEN U reverse: 5′-AAAACTCTCAACCAAACATACTAAAC ATA-3′; human PTEN M forward: 5′-GAATCGATTTGGAGTTCGAG-3′; human PTEN M reverse: CTCAACCGAACGTACTAAACGTAA-3′. The PCR product was resolved on a 1.4% agarose gel.

2.11. Production of shRNA lentiviral particle and LX-2 cells transduction

Bacterial stocks plasmids encoding sh-DNMT3B, sh-PTEN (Cat. #TRCN0000437183 and TRCN0000002747), non-targeting shRNA (pLKO.1), PCD/NL-BH4 packaging and pLTR-

G envelop plasmids were purchased from Sigma-Aldrich (St. Louis, MO). Production of shRNA lentivirus and transduction of cell lines were carried out as described previously [34]. LX-2 cells were transduced with concentrated and purified lentiviral particles (MOI = 5) in the presence of polybrene (5 μg/ml). The infected cells were cultured in complete growth medium for 72 h, and stable clones were selected with puromycin dihydrochloride (10 μg/ml). Survived colonies were pooled and expanded in complete cell culture medium containing puromycin (2 μg/ml) for further experiment.

2.12. Statistical analyses

All data are expressed as the mean ± standard error (SE) from 3 to 4 separate experiments. The differences between groups were analyzed using a two-tailed Student t-test when only two groups were analyzed or analysis of variance (ANOVA) when there were more than two groups were analyzed. The statistical analyses were conducted using the Excel (Microsoft office 2015), Graph-Pad Prism software version 5.04 (GraphPad® Software, San Diego CA). A P value < 0.05 was considered as statistically significant differences.

3. Results

Adiponectin attenuates liver fibrosis in CCl_4-treated mice and modulates PTEN expression in WT mice.

In order to examine the role of adiponectin in PTEN expression, we utilized eight-week-old WT C57BL/6 J mice treated with CCl_4 for 6 weeks to induce liver fibrosis. We also administered recombinant-deficient adenovirus carrying cDNA of adiponectin (Ad-Adipo), and control adenovirus (Ad-LacZ) at week 4 for 2 weeks. Adiponectin levels were monitored by serum ELISA. Adiponectin delivery significantly increased serum adiponectin (Saline 9.8 ± 2.7 μg/ml; CCl_4 + Ad-LacZ 8.8 ± 3.4 μg/ml; CCl_4 + Ad-Adipo 18.2 ± 3.8 μg/ml). Carbon tetrachloride (CCl_4) gavaged mice resulted in prominent liver injury including hepatocyte ballooning, steatosis, necrosis, and irregular liver lobule structure relative to normal liver (Fig. 1A). However, adiponectin treatment improved the pathological changes in livers as assessed by H&E and Sirius red staining (Fig. 1A, B). Fig. 1C–D shows that adiponectin treatment resulted in both reduction of serum transaminase levels and hepatic hydroxyproline content. PTEN mRNA and protein expression were significantly reduced (~0.5 fold compared to control) in the fibrotic liver, whereas combined adiponectin and CCl_4 treatment increased PTEN expression to levels comparable to control mice (Fig. 2A, B, C, D, E). These data indicate that adiponectin treatment enhanced PTEN expression and reduced liver fibrosis.

3.1. Adiponectin treatment promotes PTEN expression in LX-2 cells

Because HSCs are primary regulators/mediators of liver fibrogenesis [35,36], we questioned whether adiponectin treatment upregulates PTEN expression specifically within this cellular subset. To address this hypothesis, we used a well-characterized immortalized human HSC cell line (LX-2). As anticipated, TGFβ1 (5 ng/ml) significantly decreased PTEN expression in vitro (Fig. 3A; 0.53 ± 0.12 fold change vs control) while co-treatment with high molecular weight recombinant adiponectin (10 μg/ml) prevented this effect (Fig. 3A; 1.20

± 0.11 fold change vs 0.53 ± 0.12 TGFβ1 treated cells). Moreover, adiponectin treatment also attenuated TGFβ1-induced α-SMA and collagen I (Fig. 3A, B). However, while adiponectin treatment alone resulted in an increasing trend in PTEN expression, this observation failed to reach statistical significance (Fig. 3A, B). Next, we employed sh-RNA-mediated knockdown of PTEN (nearly 50% PTEN knockdown compared to scrambled sh-RNA pLKO.1) and treated the cells with TGFβ1 for 30 min, followed by Western blot analysis. TGFβ1 treatment induced AKT phosphorylation in control sh-pLKO.1-treated cells (Fig. 4A; 2.51 ± 0.12 fold change vs control) while AKT was phosphorylated in PTEN knockdown LX-2 cells in both the presence and absence of TGFβ1 (Fig. 4A; ~ > 2 fold change in sh-PTEN knockdown cells with or without TGFβ1 vs sh-pLKO.1 control). Since AKT phosphorylation is directly linked to cell survival and activation of α-SMA in HSCs [37–39]. We performed cell proliferation assays to determine whether knockdown of PTEN induced cell proliferation in LX-2 cells. We found that knockdown of PTEN promotes LX-2 cell proliferation compared to sh-pLKO.1 (Fig. 4C; 1.72 ± 0.18 mean optical density vs sh-pLKO.1 1.13 ± 0.12).

3.2. Adiponectin treatment attenuates DNMT3B expression and PTEN promoter methylation in vivo and in vitro

Previous studies have shown that PTEN promoter methylation can directly reduce PTEN expression in HSCs [20,22,31]. We examined DNMT expression in mouse liver by Western blot and qRT-PCR, and found that DNMT1, DNMT3A, and DNMT3B expression was significantly increased in CCl_4-treated fibrotic liver (Fig. 5A; ~4 fold change vs controls). Adiponectin treatment, however, caused a significant reduction of DNMT3B expression in liver lysate (Fig. 5A, B, C; protein expression 1.26 ± 0.28 in CCl_4 + Ad-adipo fold change vs 8.62 ± 0.95 CCl_4 + Ad-LacZ; mRNA expression 2.66 ± 1.08 in CCl_4 + Ad-adipo fold change vs 8.62 ± 0.95 CCl_4 + Ad-LacZ). As anticipated, CCl_4-treatment induced PTEN promoter methylation, and adiponectin treatment reduced PTEN methylation to levels comparable to control mice (Fig. 5D). Similarly, in vitro data suggest that only DNMT3B expression was significantly reduced in the presence of adiponectin (Fig. 6A, B). Adiponectin treatment reduced PTEN promoter methylation in LX-2 cells (Fig. 6C). Culture-activated primary rat HSCs were also found to highly express all forms of DNMTs compared to freshly isolated, quiescent HSCs (Fig. 7).

3.3. DNMT3B knockdown promotes PTEN expression in LX-2 cells

Our data indicate that TGFβ1-induced DNMT3B upregulation was significantly reduced by adiponectin; hence, we performed knockdown studies of DNMT3B via sh-RNA-mediated lentiviral vector (Fig. 8A, B; 0.17 ± 0.09 fold change DNMT3B expression in sh-DNMT3B vs sh-pLKO.1). The sh-RNA mediated DNMT3B knockdown significantly induced PTEN expression compared to sh-pLKO.1 (Fig. 8A; 1.39 + 0.10 fold change vs sh-pLKO.1). Interestingly, TGFβ1 failed to induce collagen type I and α-SMA expression in DNMT3B knockdown LX-2 cells compared to pLKO.1 LX-2 cells (Fig. 8A, B).

3.4. Adiponectin regulates miR-29b expression in LX-2 cells

MicroRNA 29b (miR-29b) is a direct regulator of DNMT3B expression [40,41]. We assessed the expression of miR-29b in LX-2 cells with or without adiponectin treatment.

The results revealed that expression of miR-29b significantly increased in adiponectin-treated LX-2 cells compared to control (Fig. 9A; 3.70 ± 0.31 fold change vs control). We further investigated the effects of miR-29b inhibitors and mimic on DNMT3B and PTEN expression in LX-2 cells. Transfection with a miR-29b inhibitor significantly induced DNMT3B (Fig. 9B, D; 2.72 ± 0.12 fold change vs control) and α-SMA protein expression in LX-2 cells compared to the controls (Fig. 9B, D; 2.95 ± 0.22 fold change vs control), whereas PTEN expression was markedly reduced (Fig. 9B, D; 0.45 ± 0.07 fold change vs control). Conversely, transfection with a miR-29b mimic significantly up-regulated PTEN expression in LX-2 cells compared to controls (Fig. 9C, E; 1.73 ± 0.17 fold change vs control), whereas DNMT3B (Fig. 9C, E; 0.51 ± 0.07 fold change vs control) and α-SMA were reduced (Fig. 9C, E; 0.36 ± 0.06 fold change vs control). These results suggest that adiponectin treatment upregulates miR-29b expression and in turn prevent DNMT3B expression in LX-2 cells. Ultimately, this process prevents PTEN downregulation and prohibits the fibrogenic response.

4. Discussion

Targeting specific molecules to combat liver fibrosis is a growing challenge in translational medicine. Significant progress has been made to elucidate molecular mechanisms related to liver fibrosis, and we now have a far better understanding of liver myofibroblast biology. While the anti-fibrotic properties of adiponectin have been well-characterized in preclinical settings [6,7,42,43], recombinant adiponectin therapy is not practical to administer to humans. Here, we investigated the potential role of adiponectin as an activator of PTEN expression that could reverse hepatic fibrosis. We report the following new observations: (i) Adiponectin treatment inhibits DNMT3B expression in vivo and in vitro; (ii) Adiponectin treatment reduced PTEN promoter methylation; (iii) Knockdown of PTEN results in hyper-activation of α-SMA: a key marker for HSCs activation; (iv) Knockdown of DNMT3B reduced α-SMA and collagen expression in HSCs; and (v) Adiponectin stimulation induced miR-29b and this increased PTEN expression. Together, our results provide a molecular explanation for a novel pathway that attenuates liver fibrosis through modulation of PTEN expression (Fig. 10).

The role of PTEN in liver fibrosis has been well documented [19,31,44,45]. PTEN can dephosphorylate PIP3 to PIP2, which can antagonize the PI3kinase signaling pathway. Reduced PTEN expression leads to PIP3 accumulation resulting in activation of PI3kinase followed by phosphorylation of AKT. AKT is a pro-cell survival protein that is well documented for its role in HSC proliferation and migration [13,46]. A recent report suggests that PTEN overexpression by adenovirus in the CCl_4-induced rat liver fibrosis model reduced serum ALT and AST while decreasing collagen deposition in the liver [47]. Here, we report that adiponectin can prevent the loss of PTEN during CCl_4-induced liver fibrosis and in activated HSCs. In contrast to our observations, adiponectin treatment transiently reduced PTEN expression in human bone marrow-derived stromal cells (hBMSC), indeed adiponectin-treatment partially induced PTEN expression in hBMSC after 2 h of treatment [48]. A possible explanation for this discrepancy could be that adiponectin PTEN expression in a time-dependent manner. PTEN expression can be regulated through several mechanisms such as promoter methylation, gene mutation, and via post-translational modifications

including phosphorylation at its C-terminus. In the current study, we saw no changes in PTEN phosphorylation status in the presence or absence of adiponectin (data not shown); however, adiponectin treatment did alter the status of PTEN promoter methylation both in vivo and in vitro.

We and others have previously shown that adiponectin exerts its beneficial effects on liver fibrosis via several signaling pathways including the phosphorylation of 5′ adenosine monophosphate-activated protein kinase (AMPK), focal adhesion kinase (FAK), Sirtuin 1 (SIRT1), protein tyrosine phosphatase 1B (PTP1B), suppressor of cytokine signaling-3 (SOCS-3), and the peroxisome proliferator-activated receptor- (PPARα) [7,8,49,50]. Recently published studies have clarified the role of miRNAs in liver fibrosis [29,30,44]. Not surprisingly, miRNAs have been shown to play both an anti-fibrogenic and a profibrogenic role depending on the genes targeted and the nature of the stimulus [20–22,31,32]. Here, we showed that adiponectin up-regulates miR-29b expression in LX-2 cells. Moreover, overexpression of miRNA-29b increased PTEN levels in LX-2 cells; conversely, the miR-29b inhibitor suppressed PTEN expression. DNMT3B levels were increased LX-2 cells transfected with a miR-29b inhibitor, whereas DNMT3B expression was reduced in LX-2 transfected with a miR-29b mimic RNA. Our data suggest the presence of a novel adiponectin/miR-29B/DNMT3B/PTEN signaling pathway. It has been recently reported that miR-29b/142–5p overexpression inhibits DNMTs expression in biliary atresia and contributes to pathogenesis by regulating interferon γ (IFN γ) [51]. Moreover, miR-29b overexpression results in decreased overall gene methylation and overexpression of IFN γ [51].

In conclusion, these studies provide novel insights for another molecular mechanism whereby adiponectin plays a very important role in attenuation of liver fibrosis via upregulation of miR-29b expression in LX-2 cells. Targeting activated HSCs is an emerging strategy for the prevention of liver fibrosis, which could lead to new anti-fibrotic treatment strategies that could eventually come to the clinic.

Acknowledgments

Abbreviations:

HSCs	hepatic stellate cell
TGFβ1	Transforming growth factor β1
PTEN	Phosphatase and tensin homolog deletion 10
DNMT	DNA methyl-transferase
ECM	extracellular matrix

α-SMA	α-smooth muscle actin
CCl$_4$	carbon tetrachloride
PTP1B	protein tyrosine phosphatase 1B
AMPK	adenosine monophosphate-activated protein kinase
SOCS-3	suppressor of cytokine signaling-3
PPARα	peroxisome proliferator-activated receptor-α
FAK	focal adhesion kinase
SIRT	Sirtuin

References

[1]. Bataller R, Brenner DA, Liver fibrosis, J. Clin. Invest 115 (2005) 209–218. [PubMed: 15690074]

[2]. Koyama Y, Brenner DA, Liver inflammation and fibrosis, J. Clin. Invest 127 (2017) 55–64. [PubMed: 28045404]

[3]. Bottcher K, Pinzani M, Pathophysiology of liver fibrosis and the methodological barriers to the development of anti-fibrogenic agents, Adv. Drug Deliv. Rev 121 (2017) 3–8. [PubMed: 28600202]

[4]. Higashi T, Friedman SL, Hoshida Y, Hepatic stellate cells as key target in liver fibrosis, Adv. Drug Deliv. Rev 121 (2017) 27–42. [PubMed: 28506744]

[5]. Schumacher JD, Guo GL, Regulation of hepatic stellate cells and fibrogenesis by fibroblast growth factors, Biomed. Res. Int 2016 (2016) 8323747. [PubMed: 27699175]

[6]. Jenke A, Schur R, Roger C, Karadeniz Z, Gruger M, Holzhauser L, Savvatis K, Poller W, Schultheiss HP, Landmesser U, Skurk C, Adiponectin attenuates profibrotic extracellular matrix remodeling following cardiac injury by up-regulating matrix metalloproteinase 9 expression in mice, Phys. Rep 5 (2017).

[7]. Kumar P, Smith T, Rahman K, Mells JE, Thorn NE, Saxena NK, Anania FA, Adiponectin modulates focal adhesion disassembly in activated hepatic stellate cells: implication for reversing hepatic fibrosis, FASEB J 28 (2014) 5172–5183. [PubMed: 25154876]

[8]. Handy JA, Fu PP, Kumar P, Mells JE, Sharma S, Saxena NK, Anania FA, Adiponectin inhibits leptin signalling via multiple mechanisms to exert protective effects against hepatic fibrosis, Biochem. J 440 (2011) 385–395. [PubMed: 21846328]

[9]. Park PH, Sanz-Garcia C, Nagy LE, Adiponectin as an anti-fibrotic and anti-in-flammatory adipokine in the liver, Curr. Pathobiol. Rep 3 (2015) 243–252. [PubMed: 26858914]

[10]. Liang Z, Li T, Jiang S, Xu J, Di W, Yang Z, Hu W, Yang Y, AMPK: a novel target for treating hepatic fibrosis, Oncotarget 8 (2017) 62780–62792. [PubMed: 28977988]

[11]. Alzahrani B, Iseli T, Ramezani-Moghadam M, Ho V, Wankell M, Sun EJ, Qiao L, George J, Hebbard LW, The role of AdipoR1 and AdipoR2 in liver fibrosis, Biochim. Biophys. Acta 1864 (2017) 700–708.

[12]. Okada-Iwabu M, Yamauchi T, Iwabu M, Honma T, Hamagami K, Matsuda K, Yamaguchi M, Tanabe H, Kimura-Someya T, Shirouzu M, Ogata H, Tokuyama K, Ueki K, Nagano T, Tanaka A, Yokoyama S, Kadowaki T, A small-molecule AdipoR agonist for type 2 diabetes and short life in obesity, Nature 503 (2013) 493–499. [PubMed: 24172895]

[13]. Malaney P, Uversky VN, Dave V, PTEN proteoforms in biology and disease, Cell. Mol. Life Sci 74 (2017) 2783–2794. [PubMed: 28289760]

[14]. Tao H, Zhang JG, Qin RH, Dai C, Shi P, Yang JJ, Deng ZY, Shi KH, LncRNA GAS5 controls cardiac fibroblast activation and fibrosis by targeting miR-21 via PTEN/MMP-2 signaling pathway, Toxicology 386 (2017) 11–18. [PubMed: 28526319]

[15]. McClelland AD, Herman-Edelstein M, Komers R, Jha JC, Winbanks CE, Hagiwara S, Gregorevic P, Kantharidis P, Cooper ME, miR-21 promotes renal fibrosis in diabetic nephropathy by targeting PTEN and SMAD7, Clin. Sci. (Lond.) 129 (2015) 1237–1249. [PubMed: 26415649]

[16]. Parapuram SK, Shi-wen X, Elliott C, Welch ID, Jones H, Baron M, Denton CP, Abraham DJ, Leask A, Loss of PTEN expression by dermal fibroblasts causes skin fibrosis, J. Invest. Dermatol 131 (2011) 1996–2003. [PubMed: 21654839]

[17]. Zhang X, Hadley C, Jackson IL, Zhang Y, Zhang A, Spasojevic I, Haberle IB, Vujaskovic Z, Hypo-CpG methylation controls PTEN expression and cell apoptosis in irradiated lung, Free Radic. Res 50 (2016) 875–886. [PubMed: 27367846]

[18]. Zheng L, Chen X, Guo J, Sun H, Liu L, Shih DQ, Zhang X, Differential expression of PTEN in hepatic tissue and hepatic stellate cells during rat liver fibrosis and its reversal, Int. J. Mol. Med 30 (2012) 1424–1430. [PubMed: 23041795]

[19]. He L, Gubbins J, Peng Z, Medina V, Fei F, Asahina K, Wang J, Kahn M, Rountree CB, Stiles BL, Activation of hepatic stellate cell in Pten null liver injury model, Fibrogenesis Tissue Repair 9 (2016) 8. [PubMed: 27307790]

[20]. Zheng J, Wu C, Xu Z, Xia P, Dong P, Chen B, Yu F, Hepatic stellate cell is activated by microRNA-181b via PTEN/Akt pathway, Mol. Cell. Biochem 398 (2015) 1–9. [PubMed: 25148875]

[21]. Yu F, Lu Z, Chen B, Dong P, Zheng J, Identification of a novel lincRNA-p21-miR-181b-PTEN signaling cascade in liver fibrosis, Mediat. Inflamm 2016 (2016) 9856538.

[22]. Wei J, Feng L, Li Z, Xu G, Fan X, MicroRNA-21 activates hepatic stellate cells via PTEN/Akt signaling, Biomed Pharmacother 67 (2013) 387–392. [PubMed: 23643356]

[23]. Bian EB, Huang C, Ma TT, Tao H, Zhang H, Cheng C, Lv XW, Li J, DNMT1-mediated PTEN hypermethylation confers hepatic stellate cell activation and liver fibrogenesis in rats, Toxicol. Appl. Pharmacol 264 (2012) 13–22. [PubMed: 22841775]

[24]. Wilson CL, Mann DA, Borthwick LA, Epigenetic reprogramming in liver fibrosis and cancer, Adv. Drug Deliv. Rev 121 (2017) 124–132. [PubMed: 29079534]

[25]. Moran-Salvador E, Mann J, Epigenetics and liver fibrosis, Cell. Mol. Gastroenterol. Hepatol 4 (2017) 125–134. [PubMed: 28593184]

[26]. Deng Z, He Y, Yang X, Shi H, Shi A, Lu L, He L, MicroRNA-29: a crucial player in fibrotic disease, Mol. Diagn. Ther 21 (2017) 285–294. [PubMed: 28130757]

[27]. Ha M, Kim VN, Regulation of microRNA biogenesis, Nat. Rev. Mol. Cell Biol 15 (2014) 509–524. [PubMed: 25027649]

[28]. Loosen SH, Schueller F, Trautwein C, Roy S, Roderburg C, Role of circulating microRNAs in liver diseases, World J. Hepatol 9 (2017) 586–594. [PubMed: 28515844]

[29]. Ge S, Xie J, Liu F, He J, He J, MicroRNA-19b reduces hepatic stellate cell proliferation by targeting GRB2 in hepatic fibrosis models in vivo and in vitro as part of the inhibitory effect of estradiol, J. Cell. Biochem 116 (2015) 2455–2464. [PubMed: 25650006]

[30]. McDaniel K, Huang L, Sato K, Wu N, Annable T, Zhou T, Ramos-Lorenzo S, Wan Y, Huang Q, Francis H, Glaser S, Tsukamoto H, Alpini G, Meng F, The let-7/Lin28 axis regulates activation of hepatic stellate cells in alcoholic liver injury, J. Biol. Chem 292 (2017) 11336–11347. [PubMed: 28536261]

[31]. Yu F, Chen B, Dong P, Zheng J, HOTAIR epigenetically modulates PTEN ex-pression via MicroRNA-29b: a novel mechanism in regulation of liver fibrosis, Mol. Ther 25 (2017) 205–217. [PubMed: 28129115]

[32]. Li ZJ, Ou-Yang PH, Han XP, Profibrotic effect of miR-33a with Akt activation in hepatic stellate cells, Cell. Signal 26 (2014) 141–148. [PubMed: 24100264]

[33]. Cicchini C, de Nonno V, Battistelli C, Cozzolino AM, De Santis Puzzonia M, Ciafre SA, Brocker C, Gonzalez FJ, Amicone L, Tripodi M, Epigenetic control of EMT/MET dynamics: HNF4alpha impacts DNMT3s through miRs-29, Biochim. Biophys. Acta 1849 (2015) 919–929. [PubMed: 26003733]

[34]. Chopyk DM, Kumar P, Raeman R, Liu Y, Smith T, Anania FA, Dysregulation of junctional adhesion molecule-A contributes to ethanol-induced barrier disruption in intestinal epithelial cell monolayers, Phys. Rep 5 (2017).

[35]. Wang Y, Li J, Wang X, Sang M, Ho W, Hepatic stellate cells, liver innate immunity, and hepatitis C virus, J. Gastroenterol. Hepatol 28 (Suppl. 1) (2013) 112–115.

[36]. Tacke F, Weiskirchen R, Update on hepatic stellate cells: pathogenic role in liver fibrosis and novel isolation techniques, Expert Rev. Gastroenterol. Hepatol 6 (2012) 67–80. [PubMed: 22149583]

[37]. Cai CX, Buddha H, Castelino-Prabhu S, Zhang Z, Britton RS, Bacon BR, Neuschwander-Tetri BA, Activation of insulin-PI3K/Akt-p70S6K pathway in hepatic stellate cells contributes to fibrosis in nonalcoholic steatohepatitis, Dig. Dis. Sci 62 (2017) 968–978. [PubMed: 28194671]

[38]. Kao YH, Chen PH, Wu TY, Lin YC, Tsai MS, Lee PH, Tai TS, Chang HR, Sun CK, Lipopolysaccharides induce Smad2 phosphorylation through PI3K/Akt and MAPK cascades in HSC-T6 hepatic stellate cells, Life Sci 184 (2017) 37–46. [PubMed: 28689803]

[39]. Han CY, Koo JH, Kim SH, Gardenghi S, Rivella S, Strnad P, Hwang SJ, Kim SG, Hepcidin inhibits Smad3 phosphorylation in hepatic stellate cells by impeding ferroportin-mediated regulation of Akt, Nat. Commun 7 (2016) 13817. [PubMed: 28004654]

[40]. Yan MD, Yao CJ, Chow JM, Chang CL, Hwang PA, Chuang SE, Whang-Peng J, Lai GM, Fucoidan elevates MicroRNA-29b to regulate DNMT3B-MTSS1 Axis and inhibit EMT in human hepatocellular carcinoma cells, Mar. Drugs 13 (2015) 6099–6116. [PubMed: 26404322]

[41]. Yan B, Guo Q, Nan XX, Wang Z, Yin Z, Yi L, Wei YB, Gao YL, Zhou KQ, Yang JR, Micro-ribonucleic acid 29b inhibits cell proliferation and invasion and enhances cell apoptosis and chemotherapy effects of cisplatin via targeting of DNMT3b and AKT3 in prostate cancer, Onco Targets Ther 8 (2015) 557–565. [PubMed: 25784815]

[42]. Ramezani-Moghadam M, Wang J, Ho V, Iseli TJ, Alzahrani B, Xu A, Van der Poorten D, Qiao L, George J, Hebbard L, Adiponectin reduces hepatic stellate cell migration by promoting tissue inhibitor of metalloproteinase-1 (TIMP-1) secretion, J. Biol. Chem 290 (2015) 5533–5542. [PubMed: 25575598]

[43]. Marangoni RG, Masui Y, Fang F, Korman B, Lord G, Lee J, Lakota K, Wei J, Scherer PE, Otvos L, Yamauchi T, Kubota N, Kadowaki T, Asano Y, Sato S, Tourtellotte WG, Varga J, Adiponectin is an endogenous anti-fibrotic mediator and therapeutic target, Sci. Rep 7 (2017) 4397. [PubMed: 28667272]

[44]. Niu X, Fu N, Du J, Wang R, Wang Y, Zhao S, Du H, Wang B, Zhang Y, Sun D, Nan Y, miR-1273g-3p modulates activation and apoptosis of hepatic stellate cells by directly targeting PTEN in HCV-related liver fibrosis, FEBS Lett 590 (2016) 2709–2724. [PubMed: 27423040]

[45]. An J, Zheng L, Xie S, Yin F, Huo X, Guo J, Zhang X, Regulatory effects and mechanism of adenovirus-mediated PTEN gene on hepatic stellate cells, Dig. Dis. Sci 61 (2016) 1107–1120. [PubMed: 26660904]

[46]. Godena VK, Ning K, Phosphatase and tensin homologue: a therapeutic target for SMA, Signal Transduction Targeted Ther 2 (2017) 17038.

[47]. Xie SR, An JY, Zheng LB, Huo XX, Guo J, Shih D, Zhang XL, Effects and mechanism of adenovirus-mediated phosphatase and tension homologue deleted on chromosome ten gene on collagen deposition in rat liver fibrosis, World J. Gastroenterol 23 (2017) 5904–5912. [PubMed: 28932082]

[48]. Liu X, Chen T, Wu Y, Tang Z, Role and mechanism of PTEN in adiponectin-induced osteogenesis in human bone marrow mesenchymal stem cells, Biochem. Biophys. Res. Commun 483 (2017) 712–717. [PubMed: 27986563]

[49]. Jiang Z, Zhou J, Zhou D, Zhu Z, Sun L, Nanji AA, The adiponectin-SIRT1-AMPK pathway in alcoholic fatty liver disease in the rat, Alcohol. Clin. Exp. Res 39 (2015) 424–433. [PubMed: 25703252]

[50]. Tardelli M, Claudel T, Bruschi FV, Moreno-Viedma V, Trauner M, Adiponectin regulates AQP3 via PPARalpha in human hepatic stellate cells, Biochem. Biophys. Res. Commun 490 (2017) 51–54. [PubMed: 28595905]

[51]. Yang Y, Jin Z, Dong R, Zheng C, Huang Y, Zheng Y, Shen Z, Chen G, Luo X, Zheng, MicroRNA-29b/142–5p contribute to the pathogenesis of biliary atresia by regulating the IFN-gamma gene, Cell Death Dis 9 (2018) 545. [PubMed: 29748604]
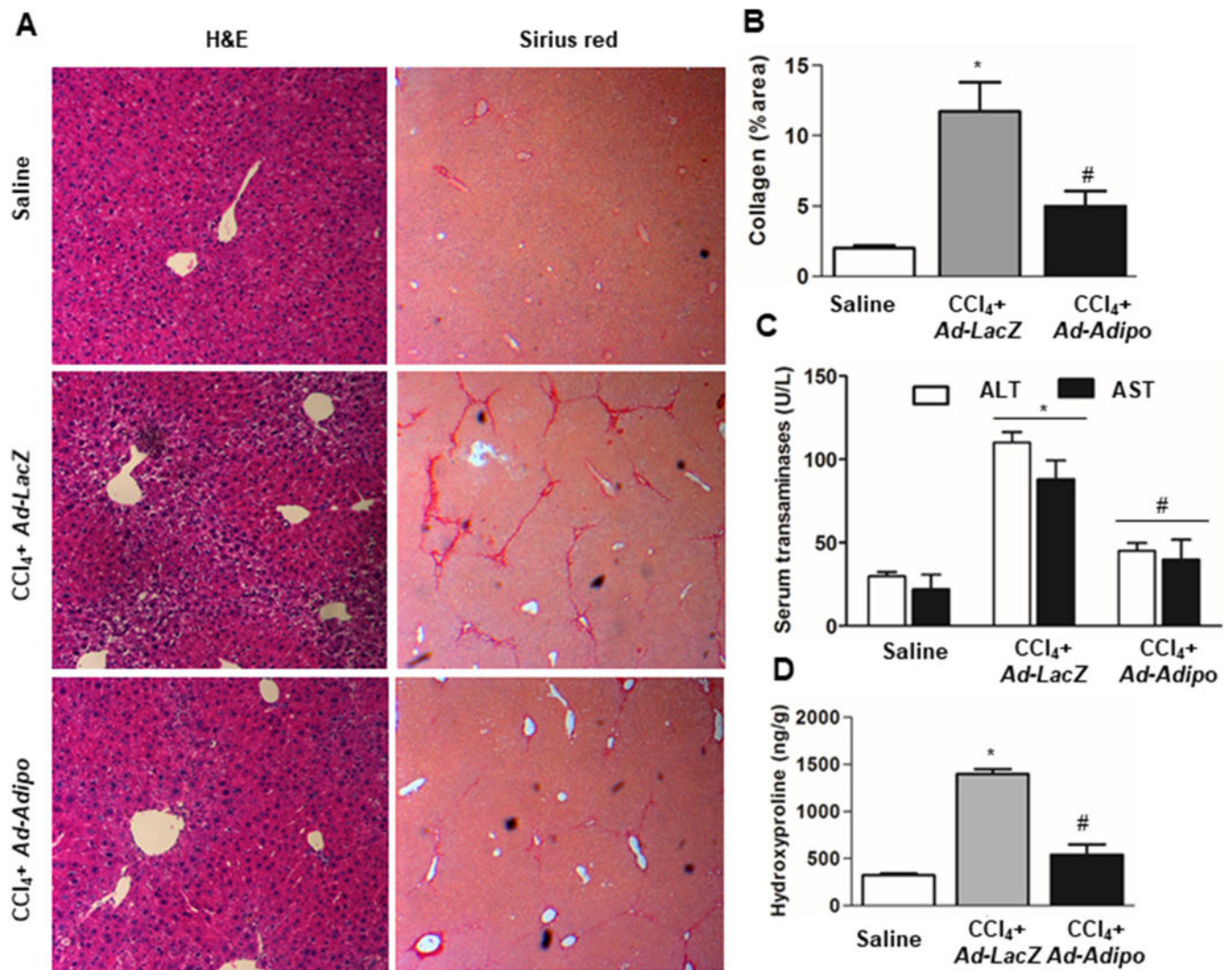
Fig. 1.
Adiponectin delivery attenuates liver fibrosis in CCl_4-treated WT mice. (A) Representative photomicrographs of H&E (left panel) and Sirius red (right panel) stained liver sections from three different groups (n = 4 in each group). (B) Quantification of Sirius red staining of sections in Fig. 1A (right panel) from all experimental mice (n = 4 in each group). (C) Serum transaminases. (D) Hepatic hydroxyproline. Data are presented as means ± SE. *$P^{<}$0.05 compared to the saline group, #$P^{<}$0.05 compared to the CCl_4 + Ad-LacZ group.
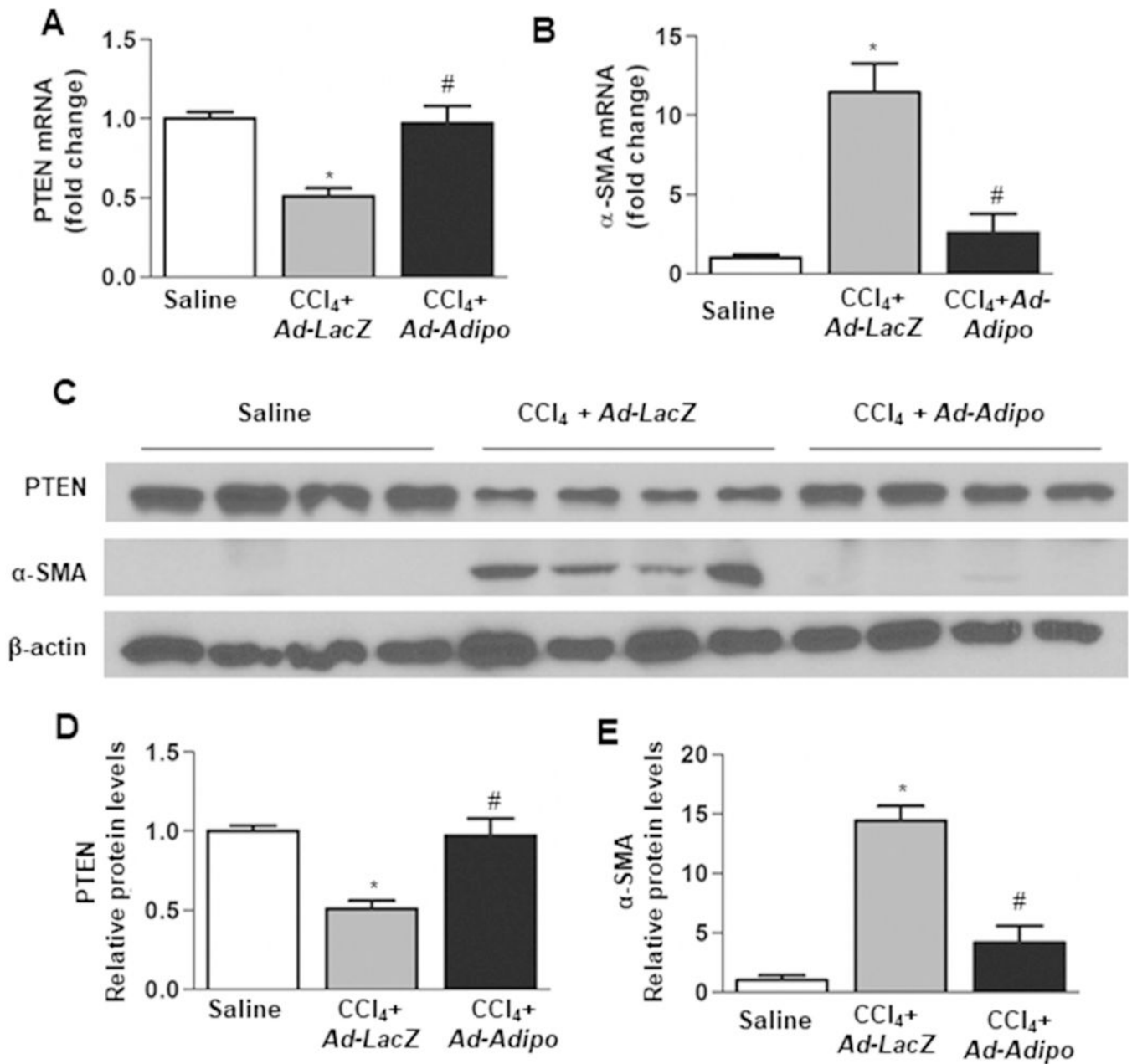
Fig. 2.
Adiponectin delivery upregulates PTEN expression in CCl_4-treated WT mice. (A, B) The mRNA levels of PTEN and α-SMA from all saline; CCl_4 + Ad-LacZ and CCl_4 + Ad-Adipo mouse livers were analyzed by qRT-PCR. (C) Western blot analysis of PTEN and α-SMA from mouse livers. (D, E) Densitometry analysis of PTEN and α-SMA expression normalized to β-actin. (n = 4 in each group). Data are presented as means ± SE. $*P < 0.05$ compared to the saline group, $\#P < 0.05$ compared to the CCl_4 + Ad-LacZ group.
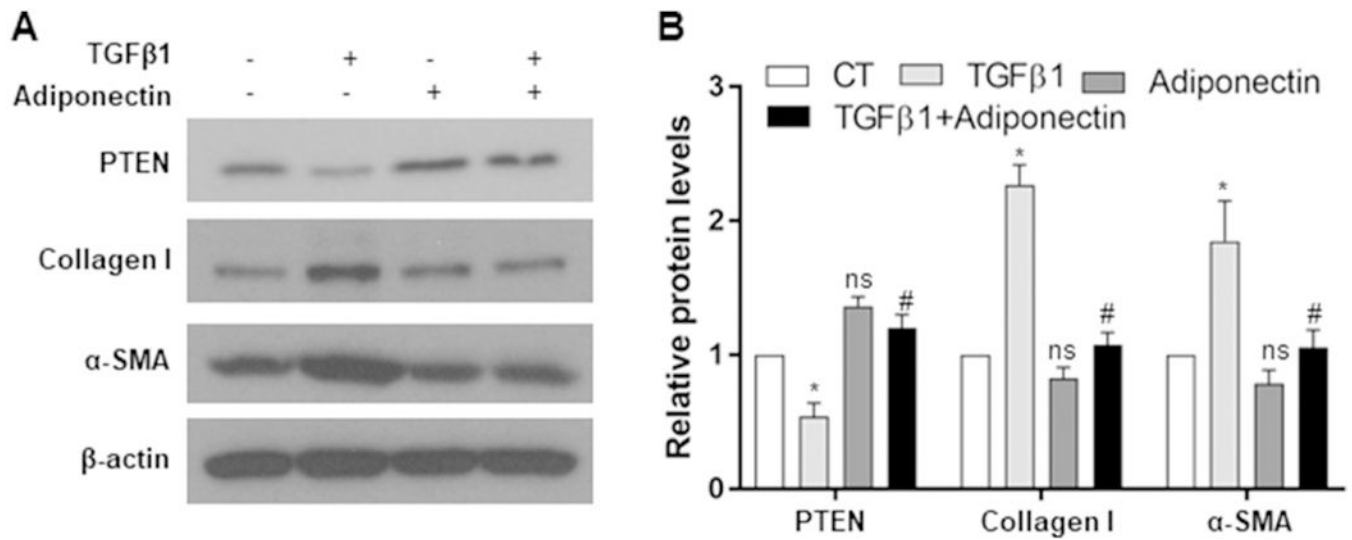
Fig. 3.
Adiponectin up-regulates PTEN expression in LX-2 cells. (A) LX-2 cells were treated either with vehicle (CT), TGFβ1, adiponectin, adiponectin and TGFβ1 together for 24 h and performed Western blot analysis. (B) Densitometry analysis of the intensity of PTEN, collagen, and α-SMA normalized to β-actin. Data are means ± SE of 4 independent experiments. *Pʹ0.05 vs control, #Pʹ0.05 vs TGFβ1 treated cells, ns = not s significantly deference compared to control.
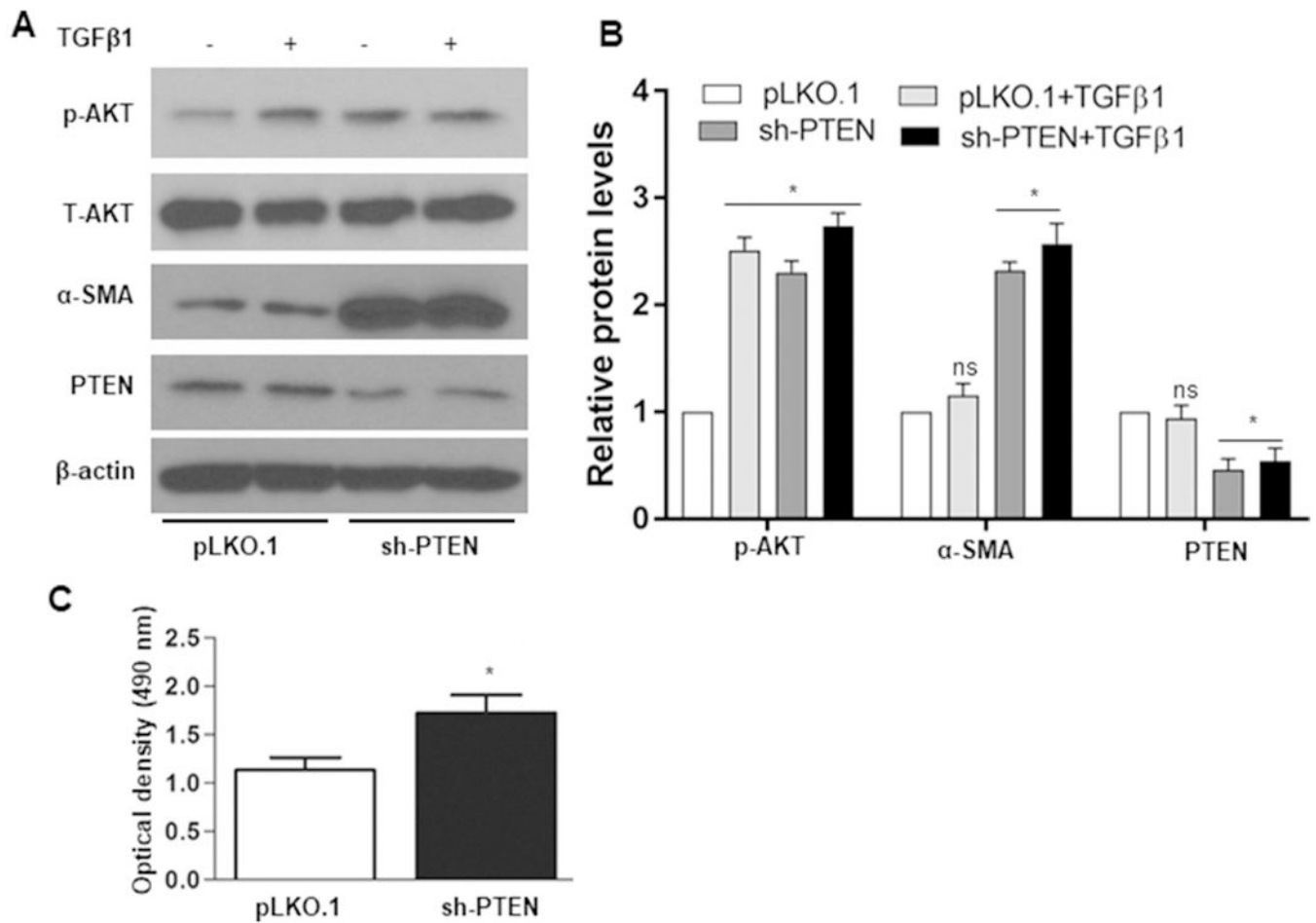
Fig. 4.
PTEN knockdown induced AKT phosphorylation and α-SMA expression in LX-2 cells. (A) sh-pLKO.1 or sh-PTEN cells were treated with TGFβ1 for 30 min followed by Western blot analysis. (B) Densitometry analysis of intensity of p-AKT normalized to total AKT. PTEN and α-SMA expression normalized to β-actin. Data are means ± SE of 3 in-dependent experiments. (C) Mean optical density of sh-PLKO.1 and sh-PTEN measured by cell titter one solution (MTS) assay. *P 0.05 vs untreated sh-pLKO.1.
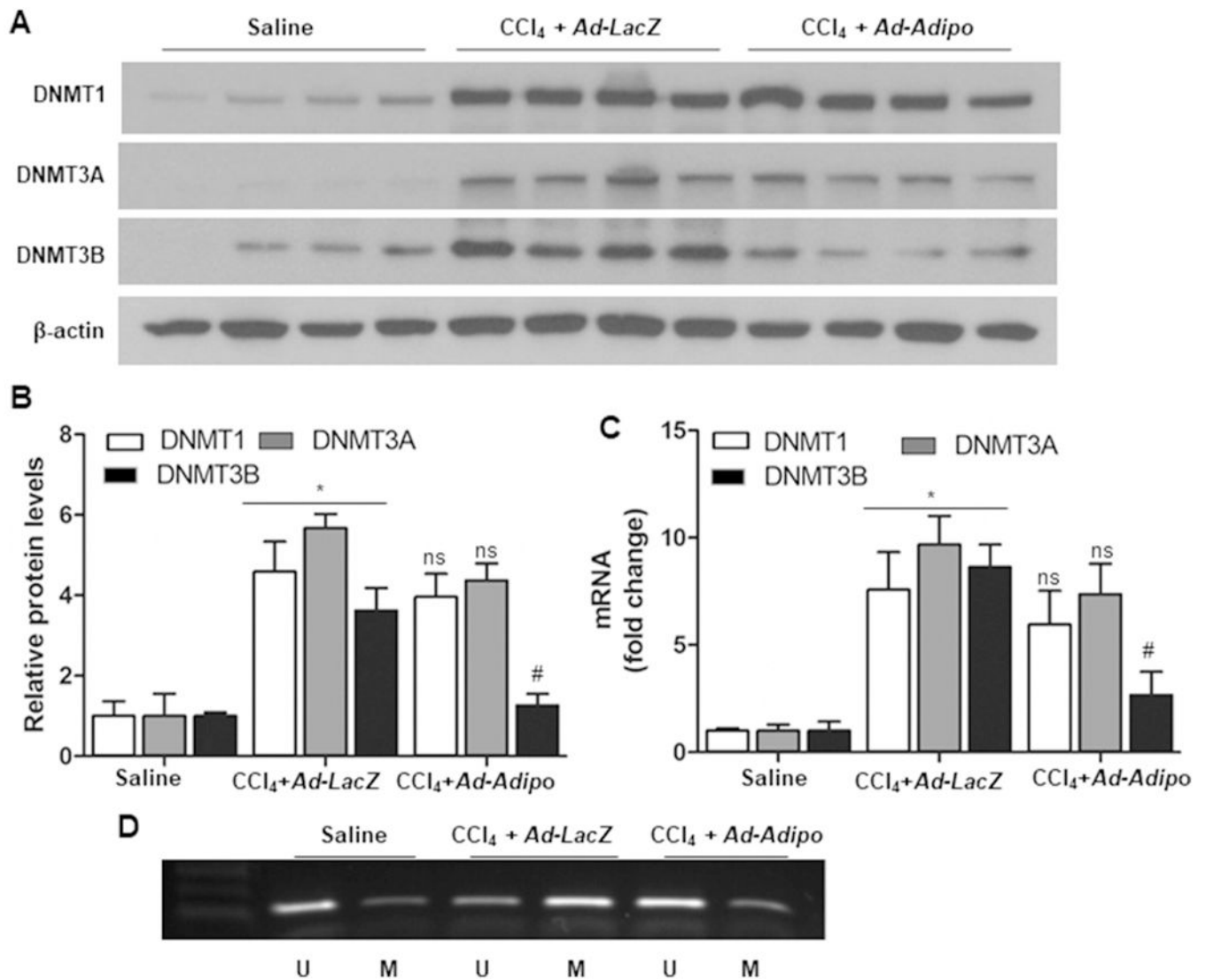
Fig. 5.
Adiponectin delivery attenuates CCl_4-induced DNMT3B expression and reduces PTEN promoter methylation in mouse liver. (A) Western blot analysis of DNMT1, DNMT3A, and DNMT3B. (B) Densitometry analysis of DNMT1, DNMT3A, and DNMT3B normalized to β-actin. (C) The mRNA levels of DMNT1, DNMT3A and DNMT3B from all saline, CCl_4 + Ad-LacZ and CCl_4 + Ad-Adipo mouse livers, respectively, were analyzed by qRT-PCR. (D) Equal amounts of bisulfite treated DNA subjected to PCR followed by agarose gel (1.4% w/v) electrophoresis. Representative image of the methylated (M) and unmethylated (U) state of PTEN promoter in liver tissue of experimental groups. The PCR product size is ~190 bp. Data are presented as means ± SE. *$P < 0.05$ compared to the saline group, #$P < 0.05$ compared to the CCl_4 + Ad-LacZ group, ns = not significantly difference between CCl_4 + Ad-LacZ and CCl_4 + Ad-Adipo group.
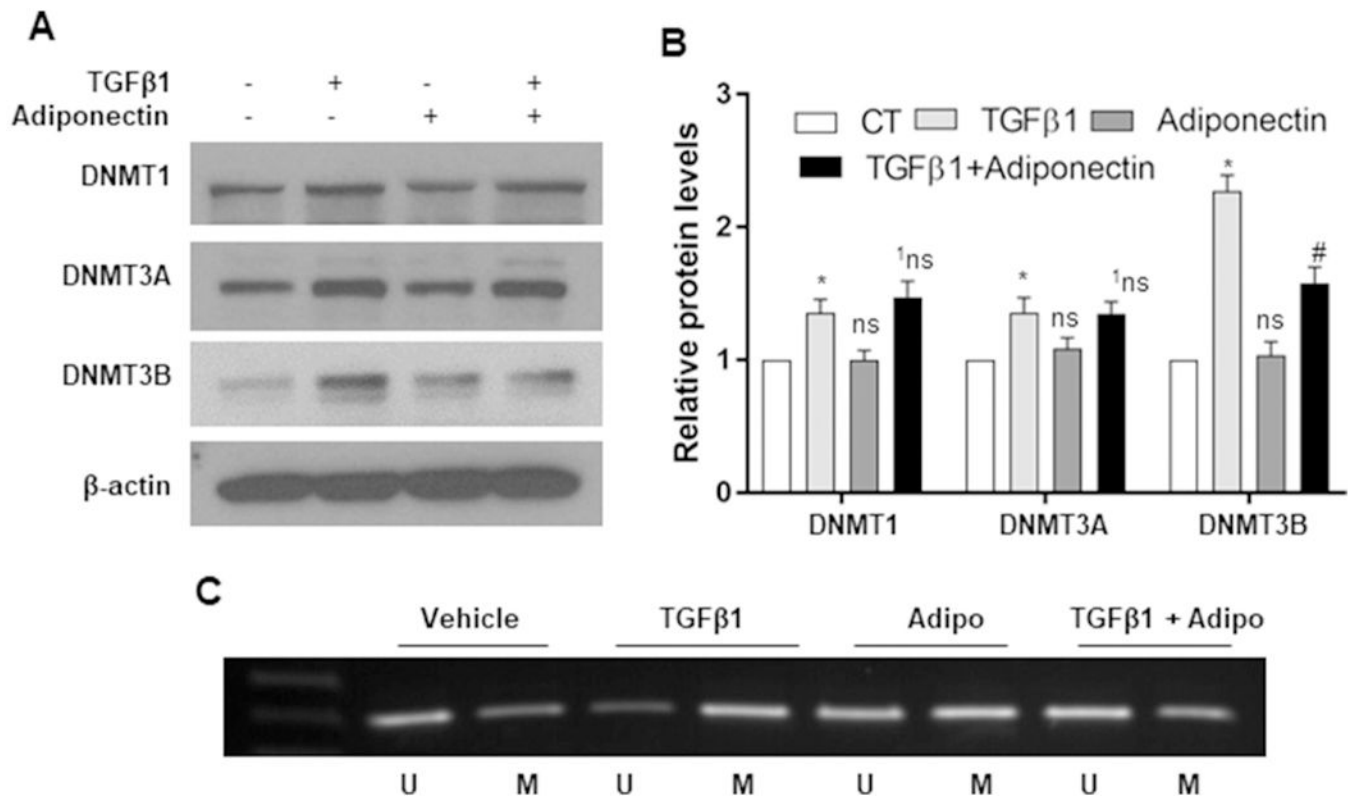
Fig. 6.
Adiponectin treatment reduced TGFβ1-induced DNMT3B expression and reduces PTEN
promoter methylation LX-2 cells. (A) Western blot analysis of DNMT1, DNMT3A and
DNMT3B in LX-2 cells. (B) Densitometry analysis of DNMT1, DNMT3A and DNMT3B
normalized to β-actin. (C) Representative image of the methylated (M) and unmethylated
(U) state of PTEN promoter in LX-2 cells. Data are means ± SE of 4 independent
experiments. *P 0.05 compared to control, #P 0.05 compared to TGFβ1 treated cells, ns =
no statistically significantly difference compared to control, [1]ns = not - significantly
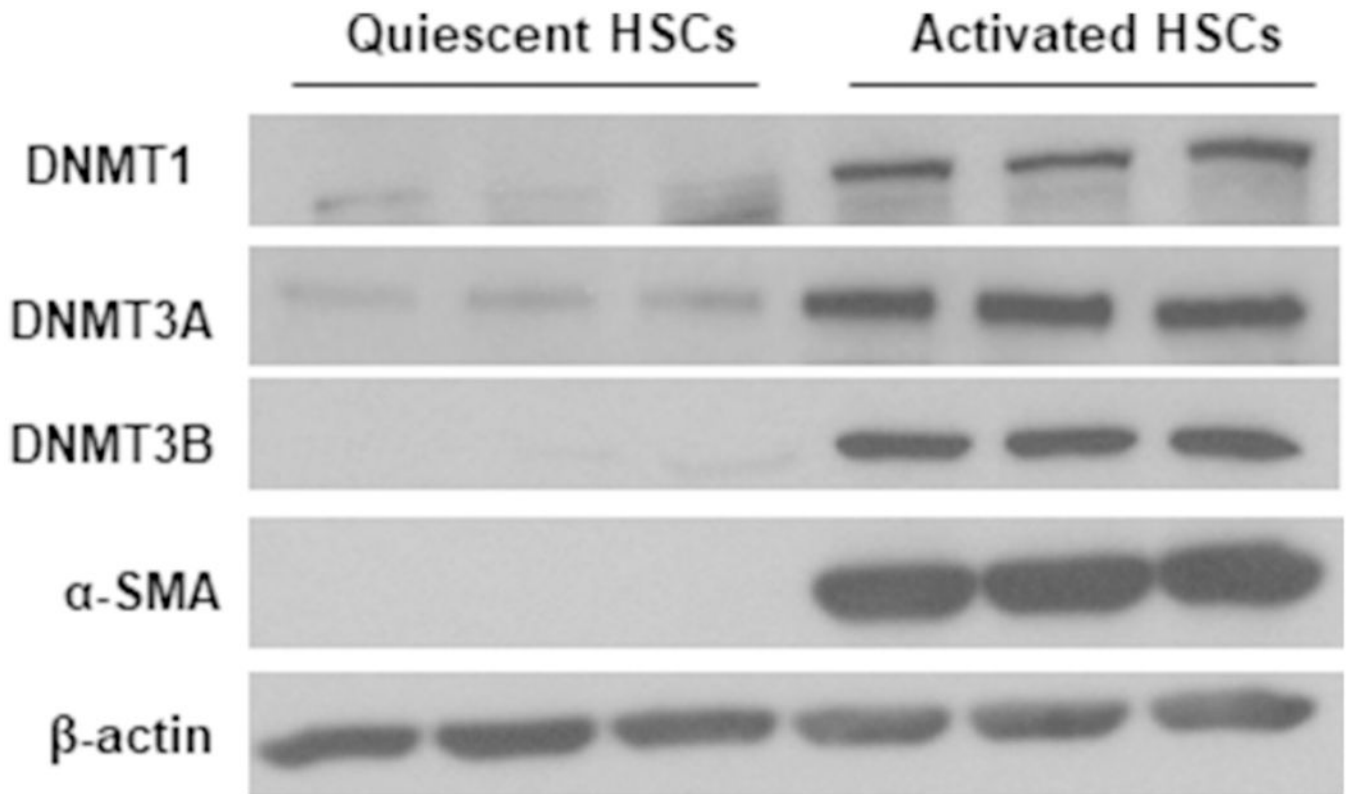difference between compared to TGFβ1 treated cells.

Fig. 7.
DNMTs expression in primary rat HSCs. DNMT1, DNMT3A and DNMT3B expression in freshly isolated HSCs (quiescent) and HSCs cultured on plastics for seven days (activated).
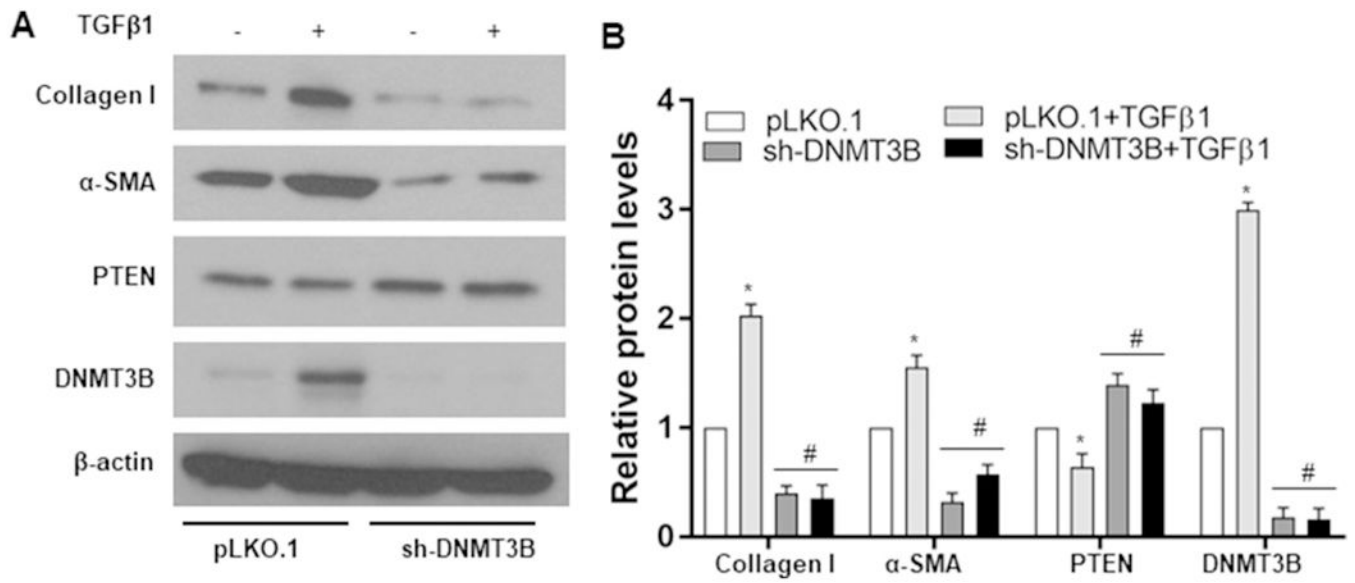
Fig. 8.
Knockdown of DNMT3B upregulates PTEN expression in LX-2 cells. (A) sh-pLKO.1 or sh-DNMT3B cells were treated with TGFβ1 for 24 h followed by Western blot analysis. (B) Densitometry analysis of the intensity of collagen I, α-SMA, PTEN, and DNMT3B expression normalized to β-actin. Data are means ± SE of 3 independent experiments. *P 0.05 vs untreated sh-pLKO.1, #P 0.05 vs sh-pLKO.1 treated with TGFβ1.
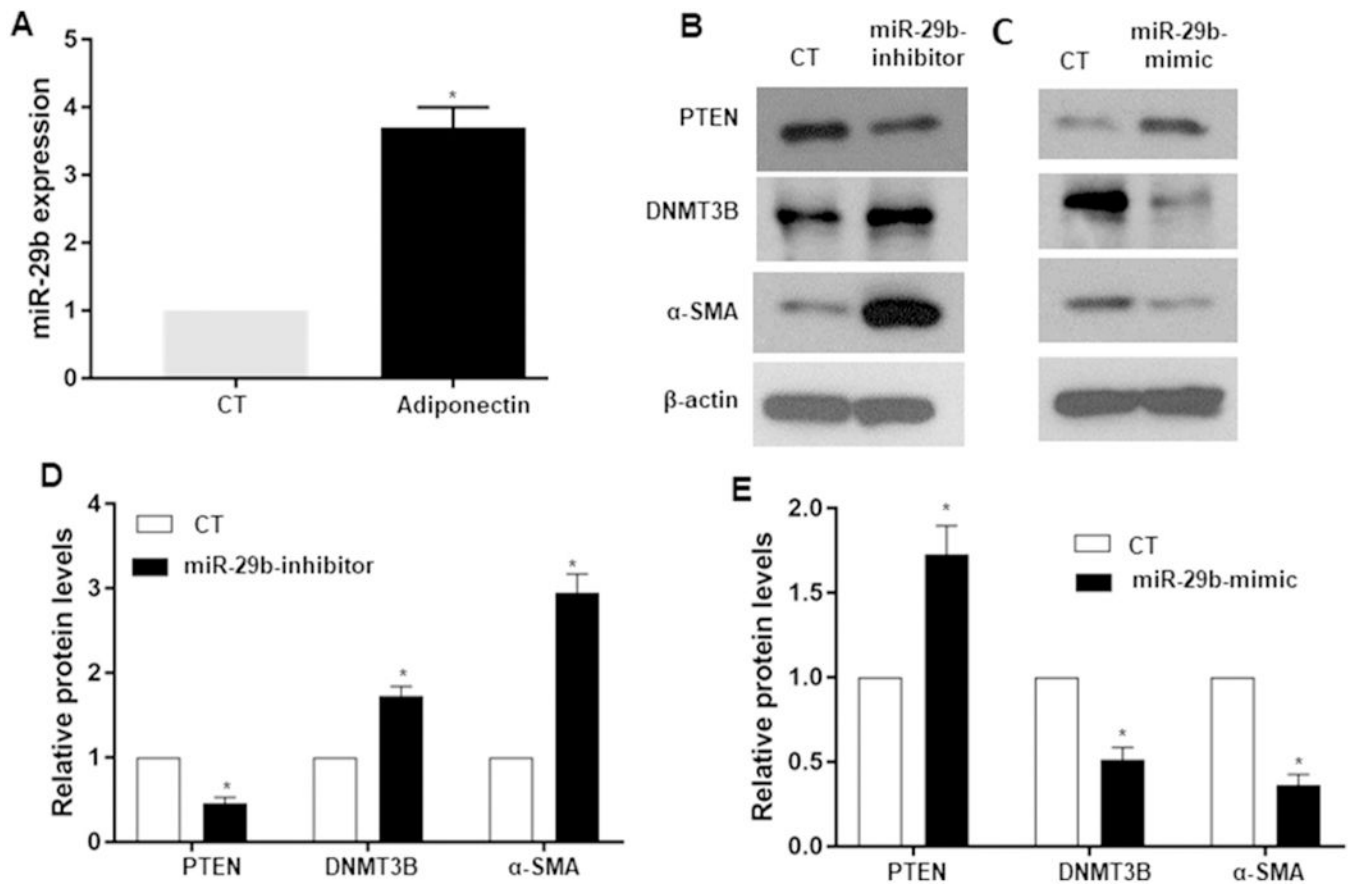
Fig. 9.
miR-29b regulates PTEN and DNMT3B expressions in LX-2 cells. (A) LX-2 cells were treated with adiponectin for 24 h and qRT-PCR was performed to measure miR-29b expression in LX-2 cells. (B, C) LX-2 cells were transfected with miR-29b inhibitor or mimic miR-29b and respective controls and performed Western blot analysis. (D, E) Densitometry analysis of the intensity of (B, C) PTEN, α-SMA, and DNMT3B expression normalized to β-actin. Data are means ± SE of 3 independent experiments. *P 0.05 vs Control.
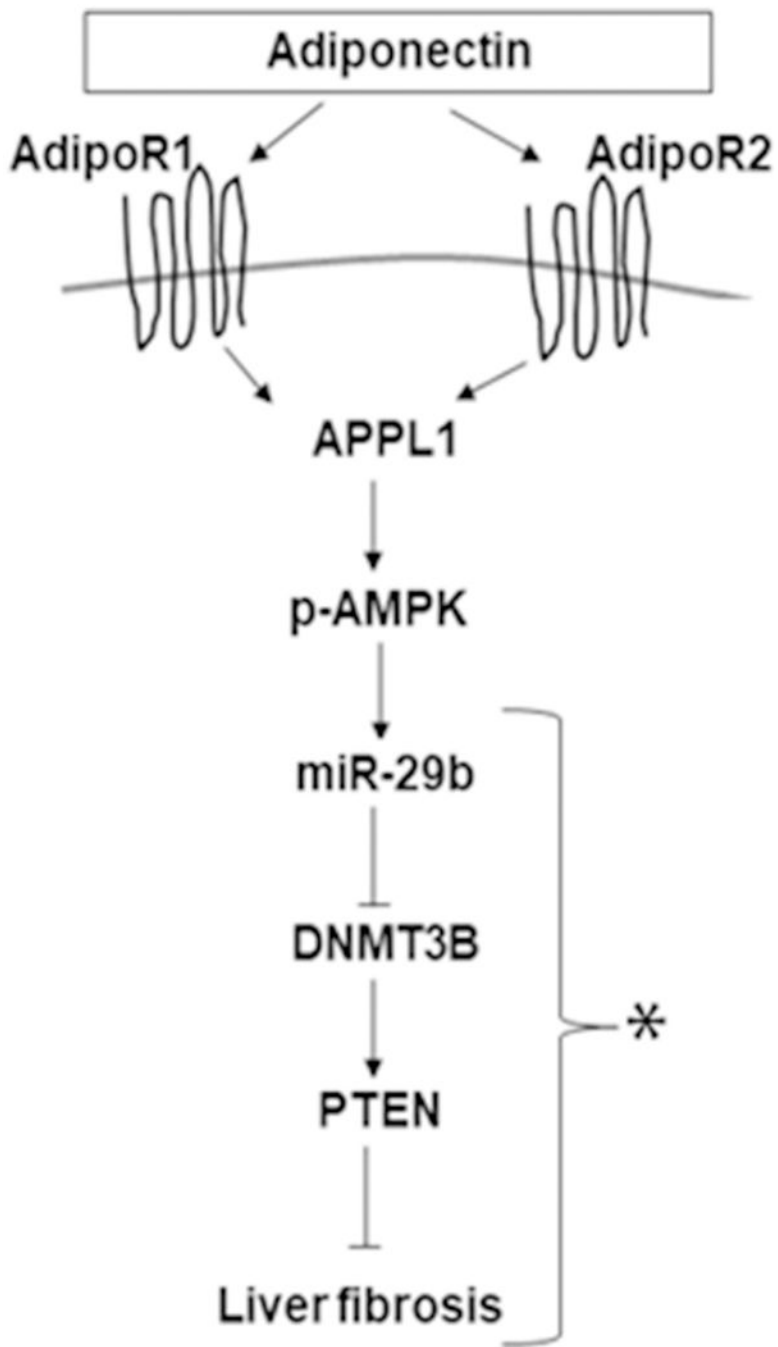
Fig. 10.
Adiponectin-mediated signaling pathway in HSCs. Adiponectin binds with adiponectin receptors (RI, R2) and induces phosphorylation of AMPK via APPL1. Adiponectin treatment induces expression of miR-29b, which leads to reduced expression of DNMT3B. The resulting reduction in DNA methylation causes upregulation of PTEN expression. Arrow-headed indicates activation, whereas bar-headed lines indicate inhibition. *novel findings of the current study.